Journal of Solid State Chemistry 269 (2019) 246–256

Contents lists available at ScienceDirect

Journal of Solid State Chemistry

journal homepage: www.elsevier.com/locate/jssc

The structures and properties of zinc(II) and cadmium(II) coordination polymers based on semi-rigid phenylenediacetate and 1,4-bis(2-methylimidazol-1-ylmethyl)benzene linkers

Güneş Günay Sezer[a,c,*], Mürsel Arıcı[b], Daniel Rixson[c], Andrew D. Burrows[c], Okan Zafer Yeşilel[b], Hakan Erer[b]

[a] Vocational School of Health Services, Bartın University, Bartın, Turkey
[b] Department of Chemistry, Eskişehir Osmangazi University, Eskişehir, Turkey
[c] Department of Chemistry, University of Bath, Claverton Down, Bath, UK

ARTICLE INFO

Keywords:
Coordination polymer
Phenylenediacetate complexes
1
4-bis(2-methylimidazol-1-ylmethyl)benzene complexes
Zinc(II) complexes
Cadmium(II) complexes

ABSTRACT

A systematic investigation into the reactions of *o*- and *p*-phenylenediacetic acid with zinc(II) and cadmium(II) salts in the presence of the semi-rigid *1,4-bis(2-methylimidazol-1-ylmethyl)benzene* (pbmeix) co-ligand is reported. Five new coordination polymers – $[Zn(\mu\text{-opda})(\mu\text{-pbmeix})_{0.5}]_n$ **1**, $\{[Zn(\mu\text{-ppda})(\mu\text{-pbmeix})]\cdot H_2O\}_n$ **2**, $\{[Zn(\mu\text{-ppda})(\mu\text{-pbmeix})]\cdot 0.5pbmeix\cdot H_2O\}_n$ **3**, $\{[Cd(\mu\text{-opda})(\mu\text{-pbmeix})]\cdot 0.5DMF\}_n$ **4** and $[Cd(\mu\text{-ppda})(\mu\text{-pbmeix})_{0.5}]_n$ **5** (o/ppda = 1,2-/1,4-phenylenediacetate) – have been prepared and structurally characterised. Compounds **1** and **5** were found to form three-dimensional coordination networks, **2** forms a two-dimensional structure whereas both **3** and **4** form one-dimensional nanotubular structures. Compounds **1** and **4** are opda complexes in which the dicarboxylate shows a tridentate coordination mode in **1** and a tetradentate coordination mode in **4**. Compounds **2**, **3** and **5** are ppda complexes in which the dicarboxylate adopts bidentate (**2**, **3**) and hexadentate (**5**) coordination modes. The structure of **2** contains interpenetrated 2D frameworks and is a polycatenane with ppda linkers from one framework passing through $Zn_2(\mu\text{-pbmeix})_2$ rings from a neighbouring framework. The thermal stability of complexes **1**–**4** and luminescence properties of complexes **1** and **4** are also reported.

1. Introduction

Coordination polymers (CPs) are compounds that are formed by linking together inorganic metal nodes with organic linkers into polymeric structures that extend in one, two, or three dimensions [1,2]. The synthesis and structural characterisation of CPs has attracted considerable interest over recent years due to the diversity of the structures and their potential uses in applications such as adsorption, gas storage, separation and catalysis, especially when porous [3–6]. The structures of CPs are dictated by the nature of both the metal centres and the organic ligands, with the reaction conditions also playing an important role: the solvent, temperature and pH influence the product in many cases [7–10]. The organic linkers, in particular, play a crucial role in determining the nature of the CP, with the number and orientation of the donor groups, ligand length and rigidity all important factors in the topology, porosity and degree of interpenetration observed [11,12].

The most commonly used organic ligands are polycarboxylates, polyphosphonates, polysulfonates and N-containing heterocycles [13]. Although most ligands employed to construct CPs are rigid, there has been increasing interest in employing semi-rigid ligands, as these allow for more variable coordination modes. In addition the absence of complete flexibility enables the formation of relatively robust and stable frameworks while maintaining the potential for porosity [14–16]. The semi-rigid 1,2-, 1,3- and 1,4-phenylenediacetate ligands have been exploited under different reaction conditions to prepare CPs with diverse structural features [5,8,17–20]. The presence of the flexible $-CH_2-$ spacers together with the rigid central aromatic ring allows for a limited degree of flexibility while still affording the potential to form open structures [19,21].

The use of a combination of anionic and neutral linkers is a well-established strategy for forming high dimensional CPs with novel topologies, and most of the CPs constructed using phenylenediacetates have been obtained by employing this approach [22–24]. We have been interested in combining semi-rigid phenylenediacetates together with semi-rigid neutral linkers, as introducing a limited degree of flexibility in both the anionic and neutral linkers maximises the potential for forming novel structures. In this paper we explore the coordination polymers formed by combining zinc(II)

* Corresponding author at: Vocational School of Health Services, Bartın University, Bartın, Turkey.
E-mail address: ggunay@bartin.edu.tr (G.G. Sezer).

https://doi.org/10.1016/j.jssc.2018.09.017
Received 26 July 2018; Received in revised form 10 September 2018; Accepted 13 September 2018
Available online 25 September 2018
0022-4596/

Table 1
Crystal data and structure refinement parameters for complexes **1**–**5**.

	1	**2**	**3**	**4**	**5**
Empirical formula	$C_{18}H_{17}N_2O_4Zn$	$C_{26}H_{28}N_4O_5Zn$	$C_{34}H_{32}N_6O_5Zn$	$C_{55}H_{59}N_9O_9\ Cd_2$	$C_{18}H_{17}N_2O_4Cd$
Formula weight	390.71	541.89	670.02	1214.91	437.74
Temperature (K)	293	150	150	293	293
Crystal system	Monoclinic	Triclinic	Triclinic	Monoclinic	Monoclinic
Space group	*P21/c*	*P*–1	*P*–1	*P21/c*	*C2/c*
a (Å)	13.7865(13)	9.2704(4)	10.4732(5)	8.6950(7)	15.153(3)
b (Å)	13.8110(13)	10.7601(5)	13.2111(6)	21.874(2)	16.178(2)
c (Å)	9.2555(7)	12.4572(5)	13.4186(5)	14.2320(11)	15.305(4)
α (°)	90	85.436(3)	106.497(4)	90	90
β (°)	100.674(3)	73.148(4)	109.067(4)	91.380(5)	117.687(5)
γ (°)	90	88.750(3)	100.883(4)	90	90
V (Å^3)	1731.8(3)	1185.47(9)	1599.26(13)	2706.1(4)	3322.4(11)
Z	4	2	2	2	8
D_c (g cm^{-3})	1.499	1.518	1.391	1.491	1.750
μ (mm^{-1})	1.44	1.83	0.82	0.85	1.34
Measured reflections	49,238	11,637	15,379	38,050	52,056
Independent reflections	3520	4774	8199	10,240	4120
R_{int}	0.051	0.037	0.024	0.128	0.043
S	1.17	1.03	1.06	0.94	1.18
R1/wR2	0.050/0.105	0.062/0.165	0.051/ 0.138	0.080/0.140	0.038/ 0.081
$\Delta\rho_{max}/\Delta\rho_{min}$ (eÅ^{-3})	0.42/−0.44	1.85/−0.98	1.69/ −0.89	0.83/−0.81	0.90/−0.77

or cadmium(II) centres together with a phenylenediacetate and 1,4-bis(2-methylbenzimidazol-1-ylmethyl) (pbmeix) linkers. Like the phenylenediacetates, pbmeix combines the possibility of facile rotation around the -CH_2- groups with the rigidity of aromatic rings providing a limited degree of flexibility, while also affording the potential for π···π interactions and hydrogen bonding [21,25–27]. Herein we report the synthesis, X-ray crystal structures and properties of five new coordination polymers – $[Zn(\mu\text{-opda})(\mu\text{-pbmeix})_{0.5}]_n$ **1** (opda = 1,2-phenylenediacetate), $\{[Zn(\mu\text{-ppda})(\mu\text{-pbmeix})]\cdot H_2O\}_n$ **2** (ppda = 1,4-phenylenediacetate), $\{[Zn(\mu\text{-ppda})(\mu\text{-pbmeix})]\cdot 0.5pbmeix\cdot H_2O\}_n$ **3**, $\{[Cd(\mu\text{-opda})(\mu\text{-pbmeix})]\cdot 0.5DMF\}_n$ **4** and $[Cd(\mu\text{-ppda})(\mu\text{-pbmeix})_{0.5}]_n$ **5**.

2. Experimental

2.1. Materials and measurements

All chemicals were commercially available and used without further purification with the exception of pbmeix which was prepared by a modification of a previously reported method for the synthesis of 1, 4-bis(imidazol-1-ylmethyl)benzene [28]. IR spectra for **1**, **4** and **5** were recorded on a Bruker Tensor 27 FT–IR spectrometer using KBr pellets whereas the IR spectra for **2** and **3** were recorded on a Perkin Elmer Spectrum 100 spectrometer with the sample mounted on a diamond ATR platform. Thermogravimetric analyses (TGA) for **1**–**4** were carried out with a Perkin Elmer Diamond TG/DTA and Setaram Setsy Evolution 16/18 Thermal Analyzer in a static air atmosphere with a heating rate of 10 °C/min over the temperature range of 30–700 °C. Powder X-ray diffraction patterns (PXRD) for **1**–**5** were recorded on a Rikagu Smartlab X-ray diffractometer or a Bruker AXS D8 Advance diffractometer. The photoluminescence (excitation and emission) spectra for the solid state samples were determined with a Perkin-Elmer LS-55 fluorescence spectrometer. Single crystal X-ray diffraction data for **1**, **4** and **5** were collected on a Bruker APEX-II diffractometer equipped with graphite-monochromated Mo-Kα radiation whereas those for **2** were collected on an Agilent SuperNova diffractometer using Cu-Kα radiation and those for **3** were collected on an Agilent XCalibur diffractometer using Mo-Kα radiation.

The structures were solved by direct methods using the programs OLEX2 [29] and SHELXT-2015 [30] with anisotropic thermal parameters for all non-hydrogen atoms. All non-hydrogen atoms were refined anisotropically by full-matrix least-squares methods using SHELXL-2015 [31], and structural figures were obtained using MERCURY [32]. Topological analysis was performed using ToposPro [33]. Crystal data and structure refinement parameters for the complexes are presented in Table 1. Selected bond lengths and angles are listed in Tables S1- S5. The crystallographic information files of **1**–**5** can be obtained from the Cambridge Crystallographic Data Centre (CCDC) and the compounds have the deposition numbers CCDC 1853013–1853017, respectively [34].

2.2. Synthesis

2.2.1. Synthesis of $[Zn(\mu\text{-opda})(\mu\text{-pbmeix})_{0.5}]_n$ (1)

A mixture of H_2opda (0.15 g, 0.8 mmol), $Zn(O_2CMe)_2\cdot 2H_2O$ (0.17 g, 0.8 mmol) and pbmeix (0.21 g, 0.8 mmol) was dissolved in DMF/H_2O (32 mL, v-v = 1:3) in a 45 mL Parr brand teflon-lined acid digestion bomb. This was sealed and then heated at 120 °C for 7 days, before cooling at a rate of 5 °C h^{-1} to room temperature. Colourless crystals of **1** were collected by filtration and washed with water. FTIR (KBr, cm^{-1}): 3128 w, 3059w, 3026w, 2960w, 2914w, 1631s, 1552 vs, 1440s, 1411s, 1367s, 1271m, 1153w, 723m.

2.2.2. Synthesis of $\{[Zn(\mu\text{-ppda})(\mu\text{-pbmeix})]\cdot H_2O\}_n$ (2) and $\{[Zn(\mu\text{-ppda})(\mu\text{-pbmeix})]\cdot 0.5pbmeix\cdot H_2O\}_n$ (3)

A mixture of H_2ppda (0.10 g, 0.5 mmol), $Zn(O_2CMe)_2\cdot 2H_2O$ (0.11 g, 0.5 mmol) and pbmeix (0.14 g, 0.5 mmol) was dissolved in DMF/H_2O (12 mL, v-v = 1:3) in a thick walled glass tube. This was sealed and then heated at 120 °C for 3 days, before cooling at a rate of 5 °C h^{-1} to room temperature. The solution was filtered and left for slow evaporation. After a few days, colourless crystals were collected by filtration and washed with water. From a mixture of products pure samples of **2** and **3**, as evidenced by PXRD, could be obtained. **2:** FTIR (KBr, cm^{-1}): 3510w, 3130w, 3000w, 2963w, 2914w, 1606s, 1602s, 1516 vs, 1440s, 1422s, 1364s, 1277m, 1144w, 740m. **3:** FTIR (KBr, cm^{-1}): 3424w, 3151w, 3132w, 2915w, 1638 vs, 1536w, 1521w, 1518s, 1432s, 1403s, 1309m, 1284m 1150w, 1012m, 712m.

2.2.3. Synthesis of $\{[Cd(\mu\text{-opda})(\mu\text{-pbmeix})]\cdot 0.5DMF\}_n$ (4)

A mixture of H_2opda (0.10 g, 0.5 mmol), $CdCl_2\cdot 2H_2O$ (0.090 g, 0.5 mmol) and pbmeix (0.27 g, 1 mmol) was dissolved in DMF (18 mL) was placed in a 45 mL Parr brand teflon-lined acid digestion bomb. This was sealed and then heated at 120 °C for 5 days, before cooling at a rate of 5 °C h^{-1} to room temperature. Colourless crystals of **4** were collected by filtration and washed with water. FTIR (KBr, cm^{-1}):

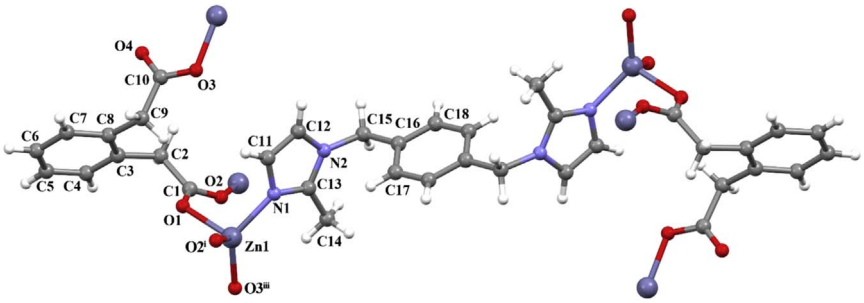

Fig. 1. Part of the structure of **1** with the atom numbering scheme showing the asymmetric unit [(i) $x, -y+{}^{1}/_{2}, z+{}^{1}/_{2}$; (iii) $-x+1, y-{}^{1}/_{2}, -z+{}^{1}/_{2}$].

3114m, 3024w, 2927w, 1679s, 1587s, 1556 vs, 1504m, 1382m, 1280w, 1002w, 775m.

2.2.4. Synthesis of {[Cd(ppda)(pbmeix)$_{0.5}$]}$_n$ (5)

A mixture of H_2ppda (0.15 g, 0.8 mmol), $Cd(O_2CMe)_2{\cdot}2H_2O$ (0.21 g, 0.8 mmol) and pbmeix (0.20 g, 0.8 mmol) was dissolved in DMF/H_2O (32 mL, v-v = 1:3) and was placed in a 45 mL Parr brand teflon-lined acid digestion bomb. This was sealed and then heated at 120 °C for 5 days, before cooling at a rate of 5 °C h^{-1} to room temperature. Colourless crystals of **5** were collected by filtration and washed with water. FTIR (KBr, cm^{-1}): 3126w, 3024w, 2943m, 1558 vs, 1510s, 1421s, 1388 vs, 1282m, 1149w, 734m.

3. Results and discussion

3.1. Syntheses

The compounds [Zn(μ-opda)(μ-pbmeix)$_{0.5}$]$_n$ **1**, {[Zn(μ-ppda)(μ-pbmeix)]·H_2O}$_n$ **2** and {[Zn(μ-ppda)(μ-pbmeix)]·0.5(pbmeix)·H_2O}$_n$ **3** were prepared as single crystals through the reactions between zinc(II) acetate, 1,2- or 1,4-phenylenediacetic acid (H_2opda/H_2ppda) and 1,4-bis(2-methylimidazol-1-ylmethyl)benzene (pbmeix) in DMF/water on heating at 120 °C for 3–7 days. For the analogous cadmium systems, the reaction between cadmium(II) acetate, H_2ppda and pbmeix gave [Cd(μ-ppda)(μ-pbmeix$_{0.5}$]$_n$ **5** under similar conditions after 5 days, but the reaction with H_2opda gave only a non-crystalline precipitate under these conditions. However, on changing the cadmium source to cadmium(II) chloride and the solvent to DMF, single crystals of {[Cd(μ-opda)(μ-pbmeix)]·0.5DMF}$_n$ **4** were formed after 5 days at 120 °C. The PXRD patterns for compounds **1**–**4** (Fig. S1-S4) were found to match well with those simulated from their single crystal X-ray structures, indicating the phase purities of the complexes. However, PXRD patterns of the bulk material of compound **5** indicate that the material is not phase pure (Fig. S5), with the compound identified crystallographically being present as a minor component in the bulk material. The reaction was repeated using a variety of different conditions, but in all cases the product contained a mixture of phases.

3.2. X-Ray crystallographic analysis

3.2.1. [Zn(μ-opda)(μ-pbmeix)$_{0.5}$]$_n$ (1)

Compound **1** was formed from reaction of zinc(II) acetate with H_2opda and pbmeix in DMF/water at 120 °C. The compound crystallises in the monoclinic space group *P*21/*c* and the asymmetric unit contains one zinc(II) centre, one opda ligand and half a pbmeix ligand (Fig. 1). The zinc centre is four-coordinate, bonding to three oxygen atoms from three different opda ligands and one nitrogen atom from the pbmeix ligand. It exhibits distorted tetrahedral geometry (τ_4 = 0.81) [35], with the bond angles ranging from 98.08(12) to 127.32(18)°. The Zn(1)–O bond distances are in the range of 1.916(3)–0.019(2) Å and the Zn(1)–N(1) bond length is 1.990(3) Å. The carboxylate group containing O(1) and O(2) bridges between zinc centres, leading to the formation of chains along the crystallographic *c* axis. These chains are connected into sheets by the opda linkers. Overall, the opda linkers adopt a μ_3-κ^1: κ^1: κ^1: κ^0

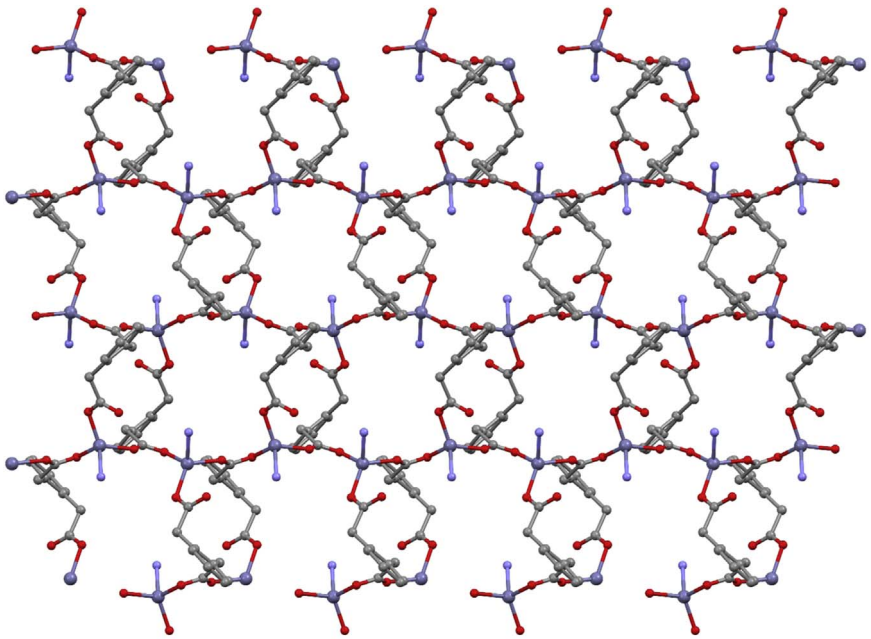

Fig. 2. The two-dimensional zinc-opda framework present in the structure of **1** viewed in the *bc* plane. Hydrogen atoms have been omitted for clarity.

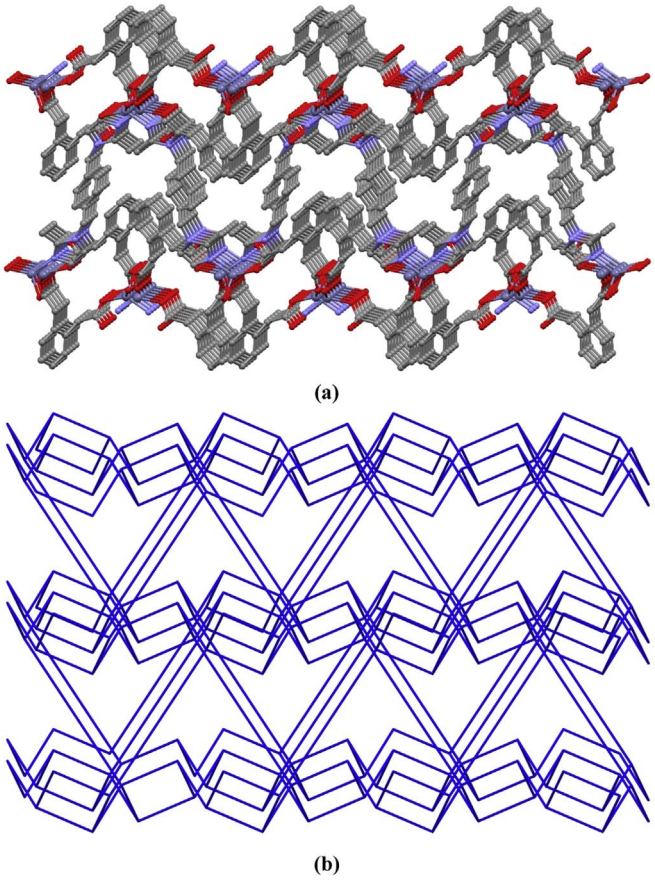

Fig. 3. (a) The 3D framework of **1**. (b) A schematic view of the binodal (3,4)-connected 3D framework topology of **1**.

coordination mode through linking the zinc centres, and the opda ligands adopt a trans conformation, constructing sheets in the *bc* plane (Fig. 2). The Zn(1)···Zn(1)^{i} and Zn(1)···Zn(1)^{ii} distances are 4.721 and 7.199 Å, respectively ((*i*) *x*, ½ − *y*, −½ + *z*, (*ii*) 1 − *x*, ½ + *y*, ½ − *z*). The distance between the zinc(II) centres bridged by the pbmeix linker is 14.303 Å. The torsion angles between the carboxylate groups and their adjacent aromatic rings are −98.64° (through C1–C2–C3–C4) and −103.02° (through C10–C9–C8–C7). Adjacent sheets are inter-linked by pbmeix ligands to generate a 3D framework (Fig. 3a). Topologic analysis reveals that complex **1** has xww-3,4-*P*21/*c* topology with the point symbol of $(4.8^2 0.10^3)(4.8^2)$ (Fig. 3b).

3.2.2. {[Zn(μ-ppda)(μ-pbmeix)]·H_2O}$_n$ (2)

Compound **2** was formed following the reaction of zinc(II) acetate with H_2ppda and pbmeix in DMF/water at 120 °C. It crystallises in the triclinic space group *P*−1, and the asymmetric unit contains one zinc(II) centre, two half ppda ligands, one pbmeix ligand and one included water molecule. As shown in Fig. 4, the Zn(II) centre is coordinated by two oxygen atoms of the carboxylate groups from two different ppda ligands and two nitrogen atoms from two different pbmeix ligands. Overall it exhibits distorted tetrahedral geometry (τ_4 = 0.92) [35], with bond angles ranging from 102.88(12) to 115.69(12)°. The Zn(1)−O(1) and Zn(1)−O(3) bond distances are 1.938(3) and 1.945(2) Å and the Zn(1)−N(1) and Zn(1)−N(4) bond lengths are 1.993(4) and 2.048 (4) Å. In contrast to **1**, there are no bridging carboxylate groups in **2**. The ppda coordinates to the metal centre through the μ_2-κ^1:κ^0:κ^1:κ^0 coordination mode, and the CH_2CO_2 groups are twisted with respect to each other in a typical trans conformation. Each ppda ligand connects two zinc(II) centres to form an infinite one-dimensional zig-zag polymeric chain, and the adjacent chains are further linked together by two different pbmeix ligands to form a 2D network in the *ab* plane (Fig. 5a and b). These sheets contain large hexagonal rings (distance across 17.8 Å) with four sides constructed from ppda ligands and two sides made from pairs of pbmeix ligands, that themselves form Zn_2(pbmeix)$_2$ rings. The Zn(1)···Zn(1)^{i} and Zn(1)···Zn(1)^{ii} distances are 12.565 and 13.743 Å, respectively ((*i*) −*x*, 1 − *y*, 2 − *z*, (*ii*) 2 − *x*, 2 − *y*, 1 − *z*). The distance between the zinc(II) centres bridged by the pbmeix linkers is 11.667 Å. These 2D layers are interpenetrated to give a 2D + 2D → 2D parallel interpenetrated structure (Fig. 6a). The interpenetration occurs when ppda ligands from one network penetrate the Zn_2(pbmeix)$_2$ rings of a neighbouring network, generating a polycatenane structure. Topologically, complex **2** is a 2-fold parallel interpenetrated 3-nodal (2,2,4)-connected 2D + 2D → 2D framework with the point symbol of (12)(4.12^5)(4) (Fig. 6b).

3.2.3. {[Zn(μ-ppda)(μ-pbmeix)]·0.5pbmeix·H_2O}$_n$ (3)

Like **2**, compound **3** was formed following the reaction of zinc(II) acetate, pbmeix and H_2ppda in DMF/water at 120 °C. It crystallises in the triclinic space group *P*−1 and the asymmetric unit (Fig. 7) contains one Zn(II) centre, one ppda ligand, one pbmeix ligand, half an uncoordinated pbmeix molecule and one included water mole-

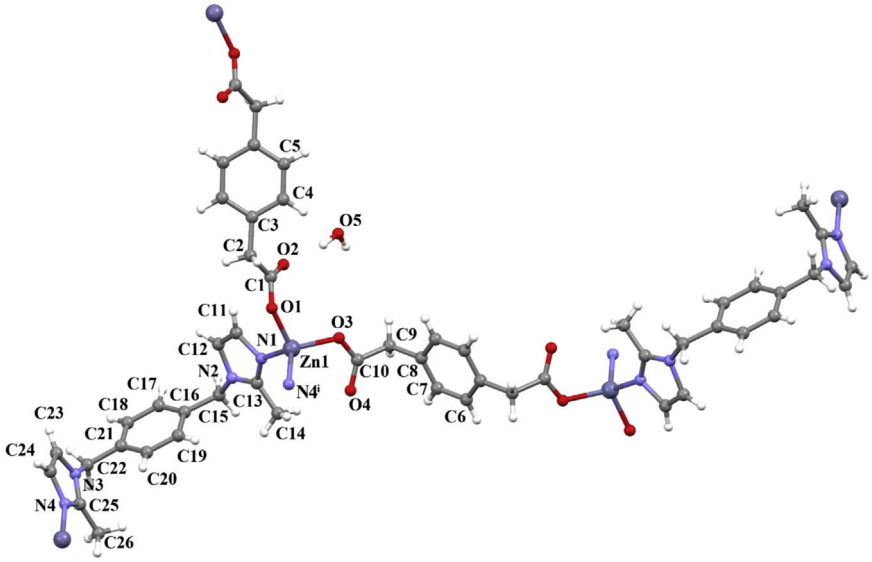

Fig. 4. Part of the structure of **2** with the atom numbering scheme showing the asymmetric unit [(i) −*x* + 2, −*y*, −*z* + 1].

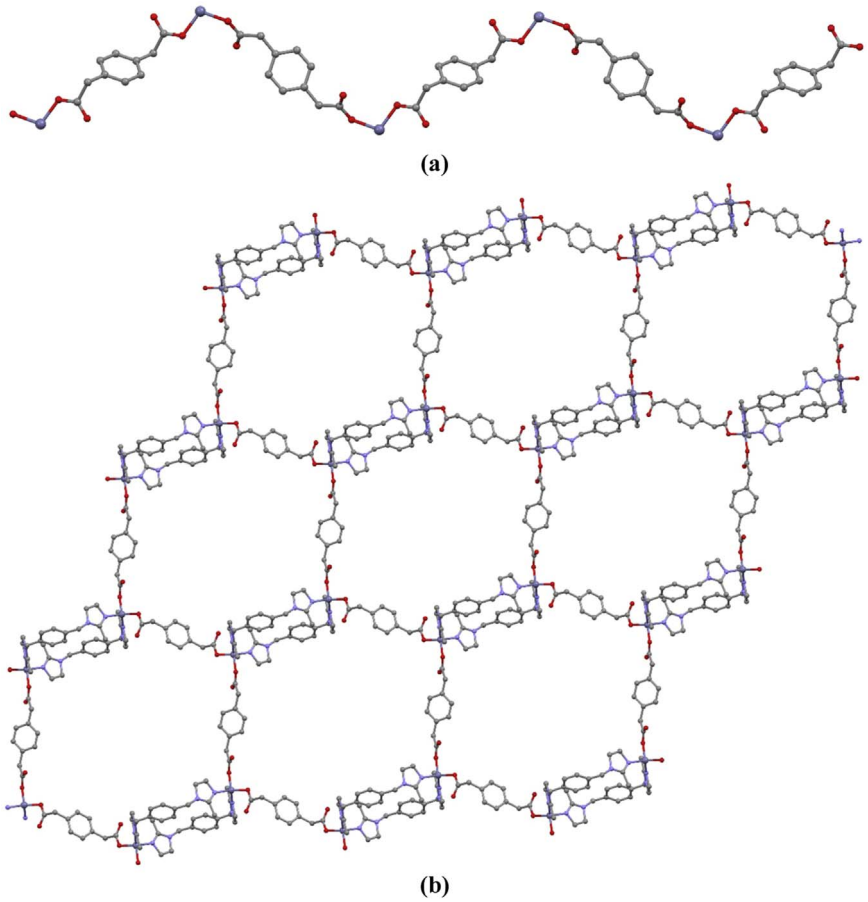

Fig. 5. The structure of **2**, showing (a) the 1D zig-zag Zn(ppda) chains and (b) the 2D sheets viewed in the *ab* plane. Hydrogen atoms and water molecules have been omitted for clarity.

cule. The Zn(II) ion is coordinated to two nitrogen atoms (N1 and N4^{ii}) from two different pbmeix ligands and two carboxylate oxygen atoms (O1 and O3^{i}) from two different ppda ligands [(i) $x+1$, y, z; (ii) $-x+2$, $-y+1$, $-z$]. Overall, it exhibits a distorted tetrahedral coordination geometry ($\tau_4 = 0.78$) [35], with the bond angles ranging from 95.76(8) to 133.49(9)°. The Zn–N bond distances are 2.024(2) and 2.020(2) Å and the Zn–O bond distances are 1.9340(19) and 1.9316(19) Å. The ppda coordinates to the Zn(II) centre through the μ_2-κ^1:κ^0:κ^1:κ^0 coordination mode, and the CH_2CO_2 groups of ppda linker are twisted with respect to each other in a trans conformation. The Zn(II) centres are connected by ppda ligands to form 1D chains (Fig. 8a), and these are inter-linked by pbmeix ligands to generate a 1D nanotubular structure (Fig. 8b) in which pairs of pbmeix ligands bridge two Zn(II) ions to form Zn_2(pbmeix)$_2$ 26-membered rings. The included, uncoordinated pbmeix molecules reside within these nanotubes, with each Zn_2(pbmeix)$_2$ ring being penetrated by a pbmeix molecule (Fig. 8c). This contrasts with the structure of **2**, as in that case the Zn_2(pbmeix)$_2$ rings were penetrated by ppda linkers. It is notable that the imidazolyl rings from neighbouring pbmeix molecules lie parallel to each other, and the short distance between them (3.547 Å) is consistent with π···π interactions. Metal-organic nanotubular structures have previously been shown to possess interesting properties and have potential applications in gas and solvent adsorption, and sensing small molecules [36–38]. Neighbouring 1D nanotubular structures and the included pbmeix and H_2O molecules are connected through hydrogen bonding, C-H···π and π···π interactions to construct a 3D supramolecular network (Fig. S6). Topologically, complex **3** is uninodal (3)-connected 1D nanotubular structure and displays SP 1-periodic net topology with the point symbol of ($4^2$0.6) (Fig. S7).

3.2.4. {[Cd(μ-opda)(μ-pbmeix)]·0.5DMF}$_n$ (4)

Compound **4** was formed from the reaction of cadmium(II) chloride with H_2opda and pbmeix in DMF at 120 °C. The topology of the structure of **4** is similar to that of **3**, despite the difference in the metal centre and phenylenediacetate. An X-ray structural analysis demonstrates that **4** crystallises in the monoclinic space group $P2_1/c$. The asymmetric unit contains one cadmium(II) centre, one opda ligand, one pbmeix ligand and half an included DMF molecule. As shown in Fig. 9, the cadmium(II) centre is six coordinate, bonding to the four oxygen atoms of two carboxylate groups, both from different opda ligands, and two nitrogen atoms from two pbmeix ligands, thus exhibiting distorted octahedral geometry. The two carboxylate groups are unsymmetrically coordinated, with that involving O(1) and O(2) being closer to being monodentate (Cd(1)–O(1) 2.233(3), Cd(1)–O(2) 2.752(4) Å) than that involving Cd(3) and Cd(4) (Cd(1)–O(3) 2.332(3), Cd(1)–O(4) 2.408(3) Å). The opda ligand coordinates to the metal centre through the μ-κ^1:κ^1:κ^1:κ^1 coordination mode, and the CH_2CO_2 groups are twisted with respect to each other in a trans conformation. The cadmium(II) centres are connected by opda ligands to form 1D chains (Fig. 10a) with a Cd(1)···Cd(1)^{i} distance of 8.695 Å ((*i*) $-1+x$, y, z). These 1D chains are connected by pbmeix ligands to generate a 1D nanotubular structure (Fig. 10b,c) that contains Cd_2(pbmeix)$_2$ 26-membered rings. Although topologically nanotubular, in practice the close

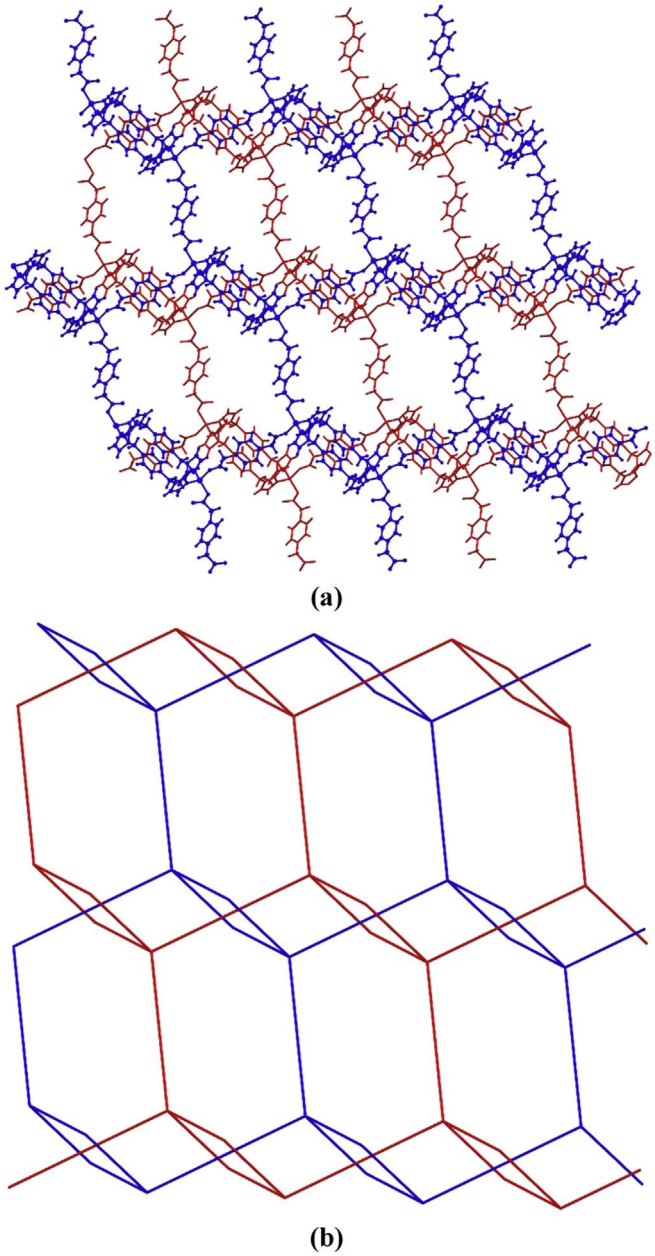

Fig. 6. (a) View of 2D + 2D → 2D parallel interpenetrated structure of **2** viewed in the *ab* plane, with hydrogen atoms omitted for clarity (b) A topologic representation of 2-fold parallel interpenetrated 2D + 2D → 2D framework.

approach of the pbmeix ligands pinch the nanotubes and lead to the formation of discrete successive pores within in the nanotubes of approximate window dimensions 6.2 × 2.9 Å. The included DMF molecules reside in these pores. The nanotubes are linked into the gross 3D supramolecular structure by a combination of C–H···π and π···π interactions. Topologically, complex **4** forms a uninodal (3)-connected 1D nanotubular structure and displays SP 1-periodic net topology with the point symbol of ($4^2$0.6) (Fig. S8).

3.2.5. [Cd(μ-ppda)(μ-pbmeix)$_{0.5}$]$_n$ (5)

Compound **5** was formed from the reaction of cadmium(II) acetate with H_2ppda and pbmeix in DMF/water at 120 °C. Single-crystal X-ray diffraction analysis reveals that **5** crystallises in the monoclinic space group *C*2/*c*. As shown in Fig. 11, the asymmetric unit of complex **5** contains one cadmium(II) centre, half a pbmeix ligand and one ppda ligand. Each cadmium(II) centre is seven-coordinate, bonding to six carboxylate oxygen atoms from four different ppda ligands and one nitrogen atom from a pbmeix ligand, and overall exhibits distorted pentagonal bipyramidal geometry. The cadmium centres are bridged by carboxylate groups into one-dimensional chains. Each of the carboxylate groups coordinates in a bidentate manner to one cadmium centre as well as bridging through one of the oxygen atoms to another cadmium centre. The bidentate modes are both unsymmetrical (Cd(1)–O(1) 2.280(2), Cd(1)–O(2) 2.652(3), Cd(1)–O(3) 2.336(3), Cd(1)–O(4) 2.664(3) Å, with the longer bond formed by the oxygen atom bridging to the second metal centre (Cd(1)–O(4)^{i} 2.355(3), Cd(1)^{ii}–O(2) 2.481(3) Å ((*i*) ½ –*x*, ½ – *y*, – *z*, (*ii*) 1 – *x*, *y*, ½ – *z*)). The ppda ligands coordinate to the metal centre through the μ_4-κ^2:κ^1:κ^2:κ^1 coordination mode and serve to link the chains into a three-dimensional (3D) framework (Fig. 12a). The CH_2CO_2 groups of ppda linker are twisted with respect to each other in a trans conformation. This structure is further stabilised by coordination of the pbmeix ligand (Fig. 12b). Topologic results show that complex **5** is a 2-nodal (4,5)-connected 3D framework with the point symbol of ($4^3$0.$6^2$0.7) ($4^3$0.$6^4$0.$7^2$0.8)(4) (Fig. 13).

4. Discussion

Comparing the metal centres in the coordination polymers **1**–**5** it can readily be seen that there is a tendency to increase the coordination numbers with the size of the metal centre. In **1**–**3**, the zinc(II) centre is four-coordinate in a distorted tetrahedral environment whereas, in contrast, in **4** and **5**, the coordination number of the larger cadmium(II) centre is six and seven respectively. This is reflected in the carboxylate coordination modes, with the carboxylates in **1**, **2** and **3**, coordinating to the zinc(II) centres through single oxygen atoms, whereas those in **4** and **5** coordinate in a bidentate manner to the cadmium(II) centres.

With respect to the phenylenediacetate ligands, all of the carboxylic

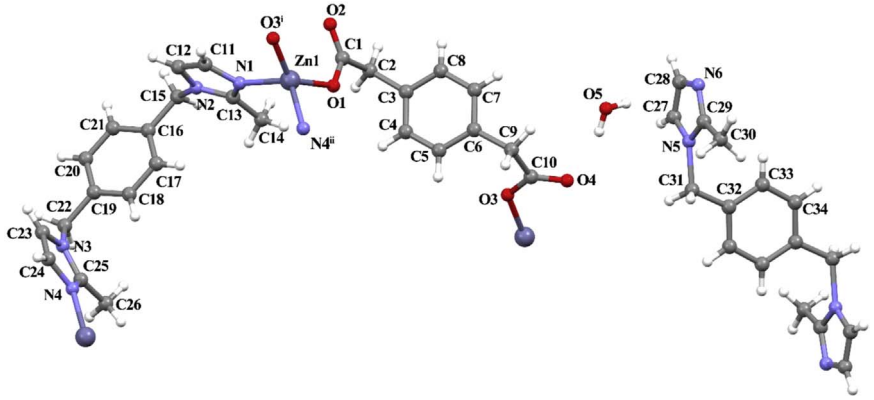

Fig. 7. Part of the structure of **3** with the atom numbering scheme showing the asymmetric unit [(i) *x* + 1, *y*, *z*; (ii) –*x* + 2, –*y* + 1, –*z*].

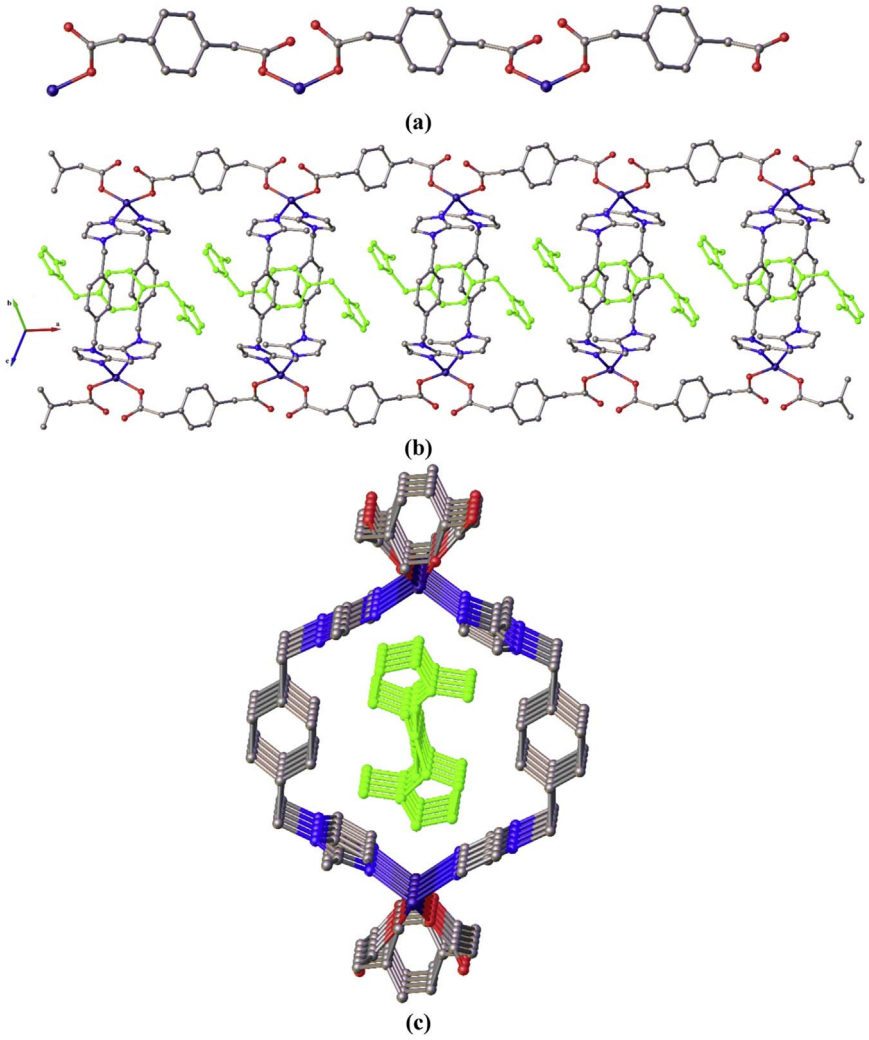

Fig. 8. The structure of **3** showing (a) a 1D polymeric chain, (b) inter-linking of the chains to form nanotubes and (c) a view down the axis of a nanotube. Hydrogen atoms have been omitted for clarity.

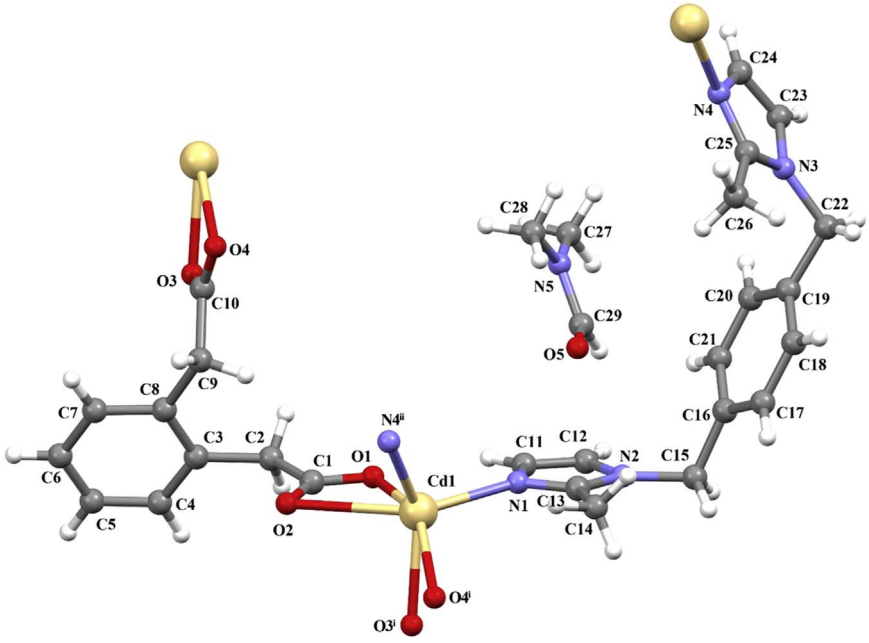

Fig. 9. Part of the structure of **4** with the atom numbering scheme showing the asymmetric unit [(i) $x+1$, y, z; (ii) $-x$, $-y+1$, $-z+1$].

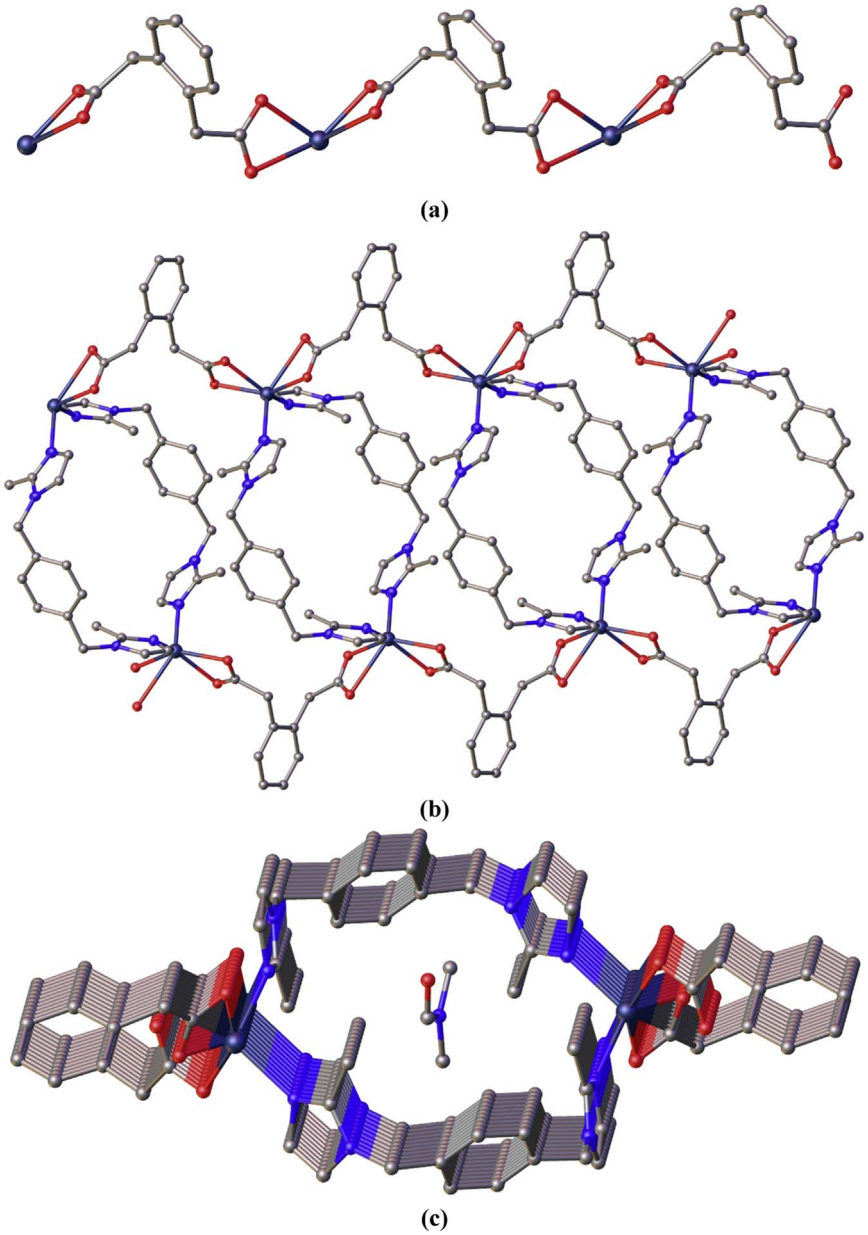

Fig. 10. The structure of **4** showing (a) the 1D polymeric Cd(opda) chains (b) the overall nanotubular structure, and (c) a view down the nanotube. Hydrogen atoms have been omitted for clarity.

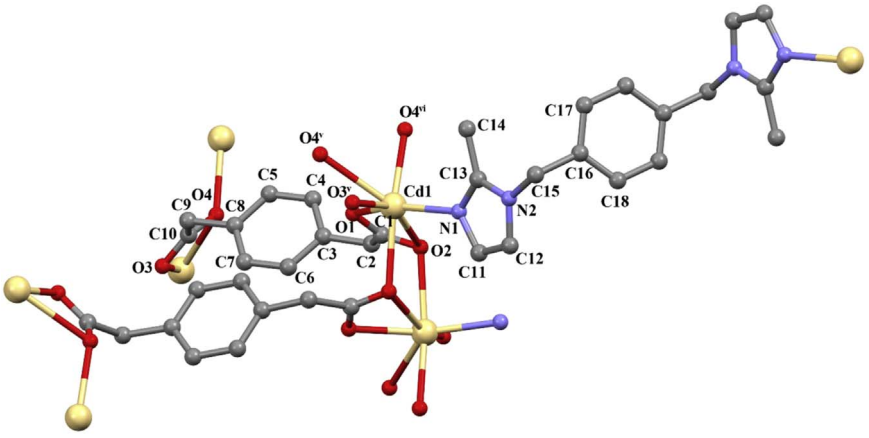

Fig. 11. Part of the structure of **5** with the atom numbering scheme showing the asymmetric unit [(v) $x, -y+1, z-{}^{1}/_{2}$; (vi) $-x+{}^{1}/_{2}, y-{}^{1}/_{2}, -z+{}^{1}/_{2}$].

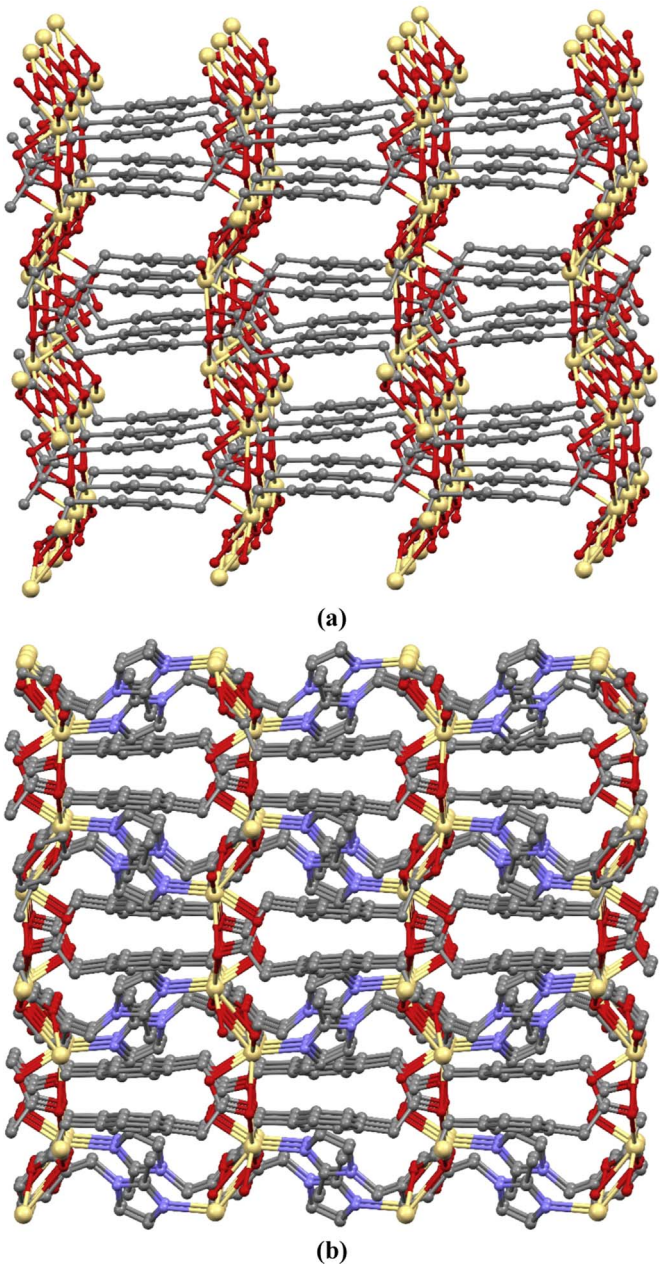

Fig. 12. The structure of **5** showing (a) the 3D structure of the Cd(ppda) framework viewed in the *bc* plane and (b) the overall 3D structure. Hydrogen atoms have been omitted for clarity.

acid groups of the H_2opda and H_2ppda reagents are deprotonated in the products. The products show four different coordination modes (Fig. 14), indicating the versatility of these linkers. For both opda and ppda, the change in metal centre leads to a change in dimensionality at the product though not in a consistent way. Thus, the Zn-opda compound **1** forms a 3D network whereas the analogous Cd-opda compound **4** forms lower dimensional 1D nanotubes. In contrast, Zn-ppda compounds **2** and **3** form a 2D network and 1D nanotubes, respectively whereas the analogous Cd-ppda compound **5** forms a higher dimensional 3D network.

It is notable that compounds **1** and **5** include only half an equivalent of pbmeix per metal centre, whereas **2** and **4** contain one equivalent of pbmeix per metal. In all cases one (or more) equivalents of pbmeix per metal ion were used in the reaction mixture and

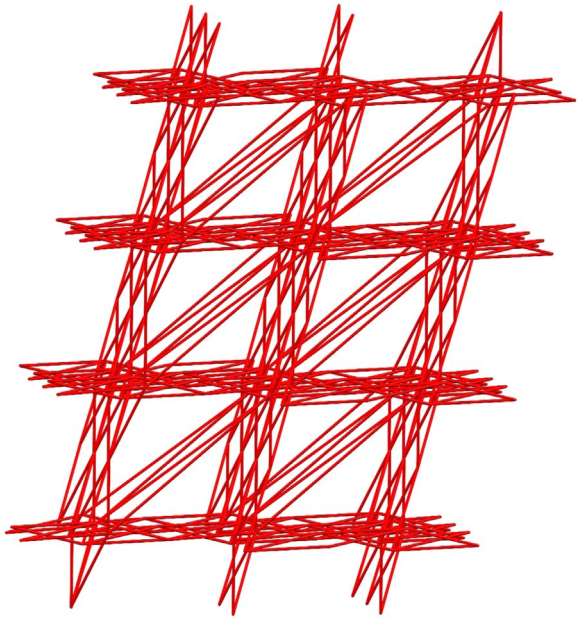

Fig. 13. A schematic view of the binodal (4,5)-connected 3D framework topology.

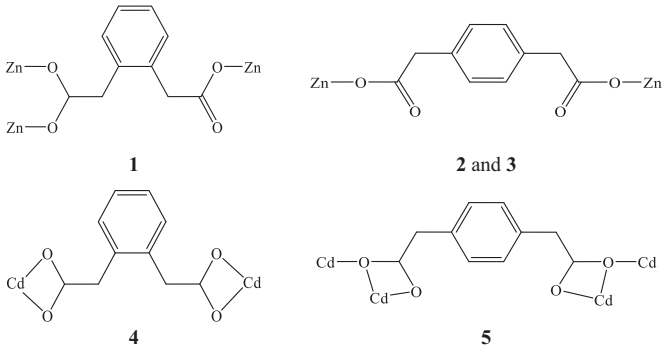

Fig. 14. The coordination modes of the o/ppda ligands in **1**–**5**.

changing the ratio of reactants does not afford other phases. In addition to coordinated pbmeix, compound **3** contains half an equivalent of included, uncoordinated pbmeix.

Zinc(II) ppda complexes with other semi-rigid *N*,*N*'-donor co-linkers have been reported previously and shown to form one- [8,39] two- [8,17,40,41] and three-dimensional [42–44] networks. Although some of the 3D networks are interpenetrated, none of the previously reported zinc ppda compounds form a polycatenane structure similar to that adopted by **2**. The network displayed by $\{[Zn(\mu\text{-ppda})(\mu\text{-mbix})]\cdot 0.5H_2O\}_n$ (mbix=1,3-bis(imidazol-1-ylmethyl)benzene) [8], contains similar sheets to those in **2**, though without the interpenetration. In contrast, the 1D chains of $[ZnCl(\mu\text{-ppda})_{0.5}(\mu\text{-mbtx})]_n$ (mbtx = 1,1'-(1,3-phenylenebis(methylene))bis(1*H*-1,2,4-triazole)) contain a similar type of catenation to that seen in **2**, despite the difference in framework dimensionality [39]. While there are previous examples of cadmium(II)-opda networks containing semi-rigid *N*,*N*'-donor co-ligands, none have similar nanotubular structures to that adopted by **4**. It is therefore clear that when using semi-rigid ligands, small changes in the ligand can have dramatic structural consequences.

4.1. Thermal properties and photoluminescence behaviour

In order to explore the thermal stabilities of the complexes, thermogravimetric analyses were undertaken on **1**–**4** under an air

atmosphere in the temperature range 30–700 °C (Fig. S9). For compounds **2** and **3**, the first mass losses in the temperature range 74–192 °C and 63–223 °C were related to removal of the included water molecules (found: 3.16%, calcd.: 3.32% for **2** and found: 3.04%, calcd.: 2.92% for **3**), respectively. Complexes **1** and **4** were stable up to 268 and 194 °C, respectively. For compound **4**, the weight loss of 10.47% in the temperature range 194–285 °C was due to removal of one DMF molecule (calcd.: 11.33%). On further heating, all complexes were fully decomposed, with the residues the oxides (ZnO, found: 19.93%, calcd: 20.73% for **1**; ZnO, found: 16.66%, calcd: 14.95% for **2**; ZnO, found: 14.96%, calcd: 13.15% for **3**, CdO, found: 21.13%, calcd: 19.94% for **4**).

The photoluminescent properties of H_2opda as well as its complexes **1** and **4** at room temperature were determined (Fig. S10). Emissions were observed at 370 and 389 nm ($\lambda ex = 292$ nm) for H_2opda, and these were attributed to $\pi^* \rightarrow \pi$ transitions. Intense broad emission peaks appeared at 389 nm ($\lambda_{ex} = 315$ nm) for **1** and 435 nm ($\lambda_{ex} = 315$ nm) for **4**. The peak shape and wavelength of the emission for the zinc(II) coordination polymer **1** are very similar to those for H_2opda, suggesting that the photoluminescence of **1** could be mainly attributed to opda ligand-centred transitions. In contrast, the emission of the cadmium(II) coordination polymer **4** is significantly red-shifted with respect to H_2opda. Similar observations in other cadmium(II) complexes have previously been attributed to LMCT processes, with the electrons promoted to the available 5*s* orbitals [45].

The emission intensities of both **1** and **4** are significantly higher than that of H_2opda so the formation of CPs enhances the fluorescence of the ligand. This is the consistent with reports on other zinc(II) and cadmium(II) complexes [46,47] which concluded that coordination of the ligand to the metal ion increases the rigidity of the ligand and reduces the loss of energy through radiation less pathways.

5. Conclusions

Five coordination polymers containing 1,4-bis(2-methylimidazol-1-ylmethyl)benzene (pbmeix) and a phenylenediacetate (opda or ppda) as linker ligands have been prepared and structurally characterised. Both the nature of the metal centre and the identity of the phenylenediacetate influence the dimensionality of the products formed, with one-, two- and three-dimensional networks all identified crystallographically. In complexes **1**–**3**, some of the oxygen atoms of o/ppda take part in coordination with zinc(II) whereas in complexes **4** and **5**, all the oxygen atoms of o/ppda coordinate to cadmium(II). Both the coordination environment of the metal ions and the bonding mode of o/ppda linkers in these coordination polymers show differences. The opda ligands in complexes **1** and **4** adopt the μ_3-κ^1:κ^1:κ^1:κ^0 tridentate and μ_2-κ^1:κ^1:κ^1:κ^1 tetradentate coordination modes whereas the ppda ligands in complexes **2**, **3** and **5** show the μ_2-κ^1:κ^0:κ^1:κ^0 bidentate and μ_4-κ^2:κ^1:κ^2:κ^1 hexadentate coordination modes, respectively. The comparison of the structures of these compounds and those with other semi-flexible ligands show that the dimensionality of **1**–**5** can be adjusted by adding a methyl group to the neutral linker. The various bonding modes and ligand conformations of opda/ppda, the methyl group of the linker pbmeix and the nature of the metal centre all play important roles in determining the structural diversity.

Acknowledgements

This work has been supported by the Research Fund of Bartın University, Turkey by Project Number: 2017-FEN-B-005.

Appendix A. Supplementary material

Supplementary data associated with this article can be found in the online version at doi:10.1016/j.jssc.2018.09.017.

References

[1] S.R. Batten, N.R. Champness, X.-M. Chen, J. Garcia-Martinez, S. Kitagawa, L. Öhrström, M. O'Keeffe, M.P. Suh, J. Reedijk, Coordination polymers, metal-organic frameworks and the need for terminology guidelines, CrystEngComm 14 (2012) 3001–3004.
[2] S.R. Batten, N.R. Champness, X.-M. Chen, J. Garcia-Martinez, S. Kitagawa, L. Öhrström, M. O'Keeffe, M.P. Suh, J. Reedijk, Terminology of metal-organic frameworks and coordination polymers (IUPAC Recommendations 2013), Pure Appl. Chem. 85 (2013) 1715–1724.
[3] F.S. Nworie, Emerging trends in coordination polymers and metal-organic frameworks: perspectives, synthesis, properties and applications, Arc Org. Inorg. Chem. Sci. 1 (2018) 39–51.
[4] S.R. Pumford, R.L. LaDuca, Nitrobenzene-detecting 2D and 3D cadmium phenylenediamine coordination polymers with *N,N'*-ethylenediaminebis(isonicotinamide) auxiliary ligands, Inorg. Chim. Acta 453 (2016) 618–625.
[5] X. Wang, J. Zhao, M. Le, H.Y. Lin, J. Luan, G. Liu, X. Wang, A Cd-coordination polymer based on a Bis-pyridyl-bis-amide ligand: synthesis, structure and its application in removal organic dyes, J. Inorg. Organomet. Polym. Mater. 28 (2018) 800–804.
[6] Q.-G. Zhai, X. Bu, X. Zhao, D.-S. Li, P. Feng, Pore space partition in metal-organic frameworks, Acc. Chem. Res. 50 (2017) 407–417.
[7] X.-Y. Dong, C.-D. Si, Y. Fan, D.-C. Hu, X.-Q. Yao, Y.-X. Yang, J.-C. Liu, Effect of N-donor ligands and metal ions on the coordination polymers based on a semirigid carboxylic acid ligand: structures analysis, magnetic properties, and photoluminescence, Cryst. Growth Des. 16 (2016) 2062–2073.
[8] G. Günay Sezer, O.Z. Yeşilel, O. Şahin, A.D. Burrows, Zinc(II) and cadmium(II) coordination polymers containing phenylenediacetate and bis(imidazol-1-ylmethyl) benzene linkers: the effect of ligand isomers on the solid state structures, J. Solid State Chem. 252 (2017) 8–21.
[9] S.R. Batten, B. Chen, J.J. Vittal, Coordination Polymers/MOFs: structures, properties and applications, ChemPlusChem 81 (2016) 669–670.
[10] G. Dikmen, O. Alver, C. Parlak, NMR determination of solvent dependent behavior and XRD structural properties of 4-carboxy phenylboronic acid: a DFT supported study, Chem. Phys. Lett. 698 (2018) 114–119.
[11] X. Zhang, L. Fan, W. Fan, B. Li, X. Zhao, Assembly of a series of d^{10} coordination polymers based on W-shaped 1,3-di(2',4'-dicarboxyphenyl)benzene: from syntheses, structural diversity, luminescence, to photocatalytic properties, CrystEngComm 17 (2015) 6681–6692.
[12] M. Arıcı, Construction, structural diversity and properties of five coordination polymers based on 5-nitroisophthalate and bis(imidazole) linkers, J. Solid State Chem. 262 (2018) 79–86.
[13] Y. Lin, C. Kong, Q. Zhang, L. Chen, Metal-organic frameworks for carbon dioxide capture and methane storage, Adv. Energy Mater. 7 (2017) 1601296.
[14] C.-D. Si, D.-C. Hu, Y. Fan, Y. Wu, X.-Q. Yao, Y.-X. Yang, J.-C. Liu, Seven coordination polymers derived from semirigid tetracarboxylic acids and N-donor ligands: topological structures, unusual magnetic properties, and photoluminescences, Cryst. Growth Des. 15 (2015) 2419–2432.
[15] K.-X. Shang, Jing-Sun, D.-C. Hu, X.-Q. Yao, L.-H. Zhi, C.-D. Si, J.-C. Liu, Six Ln (III) coordination polymers with a semirigid tetracarboxylic acid ligand: bifunctional luminescence sensing, NIR-luminescent emission, and magnetic properties, Cryst. Growth Des. 18 (2018) 2112–2120.
[16] C.-Y. Xu, S.-Y. Tang, J.-Q. Liu, D.-S. Deng, B.-M. Ji, Structural diversity and luminescent properties of two zinc(II) polymers based on semirigid N-heterocyclic ligand, Chin. J. Struct. Chem. 36 (2017) 127–134.
[17] M. Zhang, Y. Ren, Z. Ma, L. Qiao, Synthesis, crystal structure, and luminescent properties of two coordination polymers based on 1,4-phenylenediacetic acid, J. Mol. Struct. 1137 (2017) 606–609.
[18] M.-L. Zhang, Y.-J. Zheng, Z.-Z. Ma, Y.-X. Ren, J. Cao, Z.-X. Wang, J.-J. Wang, Zinc(II) and cadmium(II) complexes of long flexible bis(imidazole) and phenylenediacetate ligands, synthesis, structure, and luminescent property, Polyhedron 146 (2018) 180–186.
[19] M.-L. Zhang, D.-S. Li, J.-J. Wang, F. Fu, M. Du, K. Zou, X.-M. Gao, Structural diversity and properties of Zn^{II} and Cd^{II} complexes with a flexible dicarboxylate building block 1,3-phenylenediacetate and various heterocyclic co-ligands, Dalton Trans. (2009) 5355–5364.
[20] L.-Y. Xin, G.-Z. Liu, X.-L. Li, L.-Y. Wang, Structural diversity for a series of metal(II) complexes based on flexible 1,2-Phenylenediacetate and Dipyridyl-type coligand, Cryst. Growth Des. 12 (2012) 147–157.
[21] B.K. Tripuramallu, P. Manna, S.N. Reddy, S.K. Das, Factors affecting the conformational modulation of flexible ligands in the self-assembly process of coordination polymers: synthesis, structural characterization, magnetic properties, and theoretical studies of $[Co(pda)(bix)]_n$, $[Ni(pda)(bix)(H_2O)]_n$, $[Cu(pda)(bix)_2(H_2O)_2]_n \cdot 8nH_2O$, $[Co_2(\mu\text{-}OH)(pda)(ptz)]_n \cdot nH_2O$, $[Co(hfipbb)(bix)_{0.5}]_n$, and $[Co(2,6\text{-}pydc)(bix)_{1.5}]_n \cdot 4nH_2O$, Cryst. Growth Des. 12 (2012) 777–792.
[22] C. Xu, L. Li, Y. Wang, Q. Guo, X. Wang, H. Hou, Y. Fan, Three-dimensional Cd(II) coordination polymers based on semirigid Bis(Methylbenzimidazole) and aromatic polycarboxylates: syntheses, topological structures and photoluminescent properties, Cryst. Growth Des. 11 (2011) 4667–4675.
[23] M. Du, C.-P. Li, C.-S. Liu, S.-M. Fang, Design and construction of coordination polymers with mixed-ligand synthetic strategy, Coord. Chem. Rev. 257 (2013) 1282–1305.
[24] M.-L. Zhang, J.-J. Wang, Z.-Z. Ma, L. Qiao, Color-tunable entangled coordination polymers based on long flexible bis(imidazole) ligands and phenylenediacetate, New J. Chem. 41 (2017) 12139–12146.

[25] C. Xu, Q. Guo, X. Wang, H. Hou, Y. Fan, A case study of Zn^{II}-bmb Meso-helical coordination polymers upon the spacer angles and lengths of dicarboxylate coligands, Cryst. Growth Des. 11 (2011) 1869–1879.
[26] J.-M. Hao, Y.-N. Zhao, B.-Y. Yu, K. Van Hecke, G.-H. Cui, Structural diversity of transition-metal coordination polymers derived from isophthalic acid and bent bis(imidazole) ligands, Trans. Met. Chem. 39 (2014) 741–753.
[27] F. Semerci, Effect of substituent groups on the structures of two semi-flexible bis(imidazole) directed Zn(II)–5-sulfoisophthalate coordination polymers: syntheses, structures and photoluminescent properties, Polyhedron 139 (2018) 73–79.
[28] B.F. Hoskins, R. Robson, D.A. Slizys, An infinite 2D polyrotaxane network in $Ag_2(bix)_3(NO_3)_2$ (bix = 1,4-bis(imidazol-1-ylmethyl)benzene), J. Am. Chem. Soc. 119 (1997) 2952–2953.
[29] O.V. Dolomanov, L.J. Bourhis, R.J. Gildea, J.A.K. Howard, H. Puschmann, OLEX2: a complete structure solution, refinement and analysis program, J. Appl. Crystallogr. 42 (2009) 339–341.
[30] G.M. Sheldrick, SHELXT – Integrated space-group and crystal-structure determination, Acta Crystallogr., Sect. A 71 (2015) 3–8.
[31] G.M. Sheldrick, Crystal structure refinement with SHELXL, Acta Crystallogr., Sect. C 71 (2015) 3–8.
[32] C.F. Macrae, P.R. Edgington, P. McCabe, E. Pidcock, G.P. Shields, R. Taylor, M. Towler, J. van de Streek, Mercury: visualization and analysis of crystal structures, J. Appl. Crystallogr. 39 (2006) 453–457.
[33] V.A. Blatov, A.P. Shevchenko, D.M. Proserpio, Applied topological analysis of crystal structures with the program package topospro, Cryst. Growth Des. 14 (2014) 3576–3586.
[34] F.H. Allen, The Cambridge structural database: a quarter of a million crystal structures and rising, Acta Crystallogr. Sect. B 58 (2002) 380–388.
[35] L. Yang, D.R. Powell, R.P. Houser, Structural variation in copper(I) complexes with pyridylmethylamide ligands: structural analysis with a new four-coordinate geometry index, τ_4, Dalton Trans. (2007) 955–964.
[36] S. Ma, J.M. Simmons, D. Yuan, J.-R. Li, W. Weng, D.-J. Liu, H.-C. Zhou, A nanotubular metal-organic framework with permanent porosity: structure analysis and gas sorption studies, Chem. Commun. (2009) 4049–4051.
[37] S. Xiang, J. Huang, L. Li, J. Zhang, L. Jiang, X. Kuang, C.-Y. Su, Nanotubular Metal–organic frameworks with high porosity based on T-shaped pyridyl dicarboxylate ligands, Inorg. Chem. 50 (2011) 1743–1748.
[38] Z.-Z. Lu, R. Zhang, Y.-Z. Li, Z.-J. Guo, H.-G. Zheng, Solvatochromic BEhavior of A Nanotubular Metal–organic framework for sensing small molecules, J. Am. Chem. Soc. 133 (2011) 4172–4174.
[39] X.-J. Xu, A one-dimensional Zn^{II} coordination polymer: poly[dichlorido(μ_2-1,4-phenylenediacetato-$\kappa^2O:O'$)bis{μ_2-1,3-bis[(1*H*-1,2,4-triazol-1-yl)methyl]benzene-$\kappa^2N^3:N^{3'}$}dizinc(II)], Acta Crystallogr. Sect. C 70 (2014) 1033–1035.
[40] H.-J. Cheng, H.-X. Tang, Y.-L. Shen, N.-N. Xia, W.-Y. Yin, W. Zhu, X.-Y. Tang, Y.-S. Ma, R.-X. Yuan, Carboxylate ligands induced structural diversity of zinc(II) coordination polymers based on 3,6-bis(imidazol-1-yl)carbazole: syntheses, structures and photocatalytic properties, J. Solid State Chem. 232 (2015) 200–206.
[41] G. Günay Sezer, O.Z. Yeşilel, O. Şahin, H. Arslanoğlu, I. Erucar, Facile synthesis of 2D Zn(II) coordination polymer and its crystal structure, selective removal of methylene blue and molecular simulations, J. Mol. Struct. 1143 (2017) 355–361.
[42] J. Wang, X.-J. Xu, J.-Q. Tao, C.-Y. Tan, A fivefold interpenetrating diamond-like three-dimensional metal-organic framework: poly[(μ_2-benzene-1,4-diacetato)[μ_2-1,6-bis(1,2,4-triazol-1-yl)hexane]zinc(II)], Acta Crystallogr. Sect. C 68 (2012) m309–m311.
[43] Y.-P. Wu, D.-S. Li, J. Zhao, Z.-F. Fang, W.-W. Dong, G.-P. Yang, Y.-Y. Wang, Isomeric phenylenediacetates as modular tectons for a series of Zn^{II}/Cd^{II} coordination polymers incorporating flexible bis(imidazole) co-ligands, CrystEngComm 14 (2012) 4745–4755.
[44] G.A. Farnum, N.H. Murray, R.L. LaDuca, Parallel chain polyrotaxane, layer, and diamondoid divalent metal coordination polymers containing *para* aromatic dicarboxylate and bis(4-pyridylmethyl)piperazine ligands, Inorg. Chim. Acta 406 (2013) 65–72.
[45] S.-L. Zheng, J.-H. Yang, X.-L. Yu, X.-M. Chen, W.-T. Wong, Syntheses, structures, photoluminescence, and theoretical studies of d^{10} metal complexes of 2,2'-dihydroxy-[1,1']binaphthalenyl-3,3'-dicarboxylate, Inorg. Chem. 43 (2004) 830–838.
[46] Y. Li, H. Song, Q. Chen, K. Liu, F.-Y. Zhao, W.-J. Ruan, Z. Chang, Two coordination polymers with enhanced ligand-centered luminescence and assembly imparted sensing ability for acetone, J. Mater. Chem. A 2 (2014) 9469–9473.
[47] N. Li, H.-L. Guo, H.M. Hu, J. Song, B. Xu, M.-L. Yang, F.-X. Dong, G.-L. Xue, Hydrothermal syntheses, crystal structures and luminescence properties of zinc(II) and cadmium(II) coordination polymers based on bifunctional 3,2':6',3''-terpyridine-4'-carboxylic acid, J. Solid State Chem. 198 (2013) 416–423.